NANO LETTERS

Letter

pubs.acs.org/NanoLett

Magnetic Excitations of Rare Earth Atoms and Clusters on Metallic Surfaces

Tobias Schuh,[†] Toshio Miyamachi,[†] Stefan Gerstl,[†] Matthias Geilhufe,[‡] Martin Hoffmann,[§] Sergey Ostanin,[‡] Wolfram Hergert,[§] Arthur Ernst,[‡] and Wulf Wulfhekel*[,†]

[†]Karlsruhe Institute of Technology, Physikalisches Institut, Wolfgang-Gaede-Str. 1, 76131 Karlsruhe, Germany

[‡]Max-Planck Institut für Mikrostrukturphysik, Weinberg 2, 06120 Halle, Germany

[§]Institut für Physik, von-Seckendorff-Platz 1, Martin-Luther-Universität Halle-Wittenberg, D-06099 Halle, Germany

ABSTRACT: Magnetic anisotropy and magnetization dynamics of rare earth Gd atoms and dimers on Pt(111) and Cu(111) were investigated with inelastic tunneling spectroscopy. The spin excitation spectra reveal that giant magnetic anisotropies and lifetimes of the excited states of Gd are nearly independent of the supporting surfaces and the cluster size. In combination with theoretical calculations, we argue that the observed features are caused by strongly localized character of 4*f* electrons in Gd atoms and clusters.

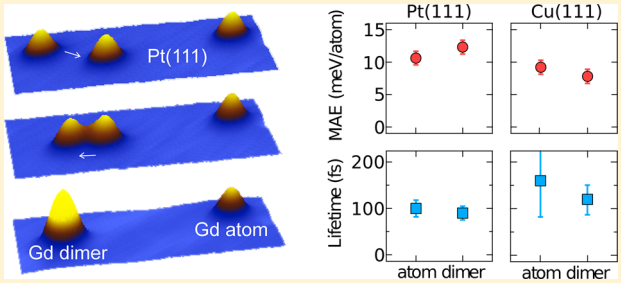

KEYWORDS: *Rare earth atoms and clusters, scanning tunneling microscopy, inelastic tunneling spectroscopy, atomic manipulation, magnetic anisotropy, magnetization dynamics*

The demand for high bit density of data storage has significantly increased in the last few decades. In the future this requires a further industrial development in combination with a fundamental understanding of spin physics in small clusters. At the heart of the stability of bits is the magnetic anisotropy. With shrinking bit size, bits require higher magnetic anisotropy energy (MAE) per atom to keep their magnetization in a specific direction against thermal fluctuations. Investigations of atomic scale nanostructures have been intensively done for transition metal atoms or clusters on metallic surfaces showing giant MAEs in the range of several meV per atom. Several important factors of the magnetic stability were identified: (i) Owing to lower atomic coordination number, the orbital momenta and the MAE per atom of a cluster increase with decreasing the size as has been demonstrated using X-ray magnetic circular dichroism (XMCD).[1] (ii) Hybridization of the 3*d* electrons of the atoms or clusters with the conduction electrons of the substrate enhances the MAE per atom by reinforcing spin orbit interaction. It, however, also lowers the lifetimes of the magnetic states due to an efficient electron−electron scattering processes induced by the strong hybridization of 3*d* states and the surface as has been deduced from inelastic tunneling spectroscopy (ITS) performed with a scanning tunneling microscope (STM).[2,3] In spite of the large MAE, transition metal atoms or clusters have a limited potential as magnetically stable bits in terms of their lifetimes on the scale of few femtoseconds. To obtain longer lifetimes of the spin states, introducing an insulating layer on surfaces is one choice to decouple clusters from surfaces, although this might spoil the advantage of enhancing the MAE with hybridization.[4−6]

An alternative path is to use 4*f* rare earth atoms instead of 3*d* transition metal atoms. As the relativistic spin orbit interaction plays a crucial role for the MAE, 4*f* atoms with larger spin (S) and orbital (L) momenta and a heavier nucleus could show larger MAEs than 3*d* atoms. Further, the strong localization of the 4*f* states leads to less hybridization with the surface, which could increase the lifetimes of the spin states. Despite these promising prospects as magnetically stable bits, magnetic properties of 4*f* rare earth atoms and clusters on surfaces have not been studied. Moreover, it is a priori not clear if the 4*f* electrons can at all be accessed in inelastic tunneling experiments.

Here we show the first study of the magnetic properties including the magnetization dynamics of rare earth Gd atoms and dimers on metallic Pt(111) and Cu(111) surfaces using an STM. Our results reveal not only that the 4*f* states can indeed be accessed with tunneling electrons but also that the strong localization of the 4*f* states suppresses the hybridization with the substrate, emphasizing the quantum nature of the spins in the shielded 4*f* orbitals of Gd.

All of the measurements were performed with a home-built low-temperature STM in ultrahigh vacuum ($p < 3 \times 10^{-11}$ mbar) at 4.3 K. An STM tip is prepared by electrochemical etching of a W wire and cleaned by subsequent flashing in vacuum. Clean Pt(111) and Cu(111) surfaces were obtained by several cycles of Ar^+ ion sputtering and annealing at 870 K for Pt(111) and at 720 K for Cu(111). A small amount (0.002

Received: June 15, 2012
Revised: July 30, 2012
Published: August 20, 2012

ML) of Gd was deposited onto Pt(111) and Cu(111) surfaces at 4.3 K by electron beam evaporation. Figure 1a and b (upper

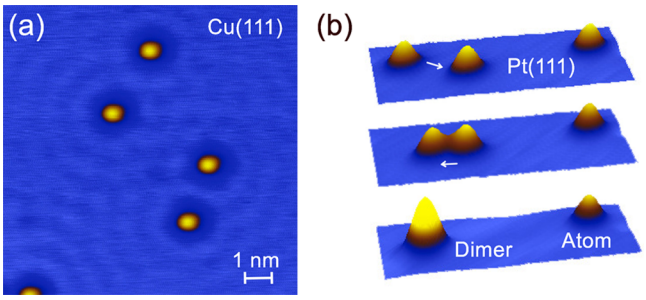

Figure 1. (a) Topography of Gd single atoms on Cu(111). The standing waves on Cu(111) are also seen in the image. (b) Creating a Gd dimer by atomic manipulation of Gd atoms on Pt(111). The sizes of 3D-STM images are 3.4 nm × 9.0 nm.

panel) shows STM images of Cu(111) and Pt(111) surfaces after Gd deposition. Due to low temperature deposition, the diffusion of Gd atoms is restricted, which results in isolated atoms. Single atoms can be laterally manipulated with the STM tip[7] (middle panel in Figure 1b) to create a dimer (bottom panel in Figure 1b). The difference between the atom and the dimer is clearly seen from their heights.

The MAE of Gd atoms was determined by detecting the inelastic spin-flip excitation with ITS. Considering the rotational symmetry, for a single atom or a dimer on surfaces, the uniaxial anisotropy with the easy axis out-of-plane is the leading term. In such a system, the MAE is described quantum mechanically as DJ_z^2 ($D < 0$) and classically as $K \cos^2 \theta$ (θ: the magnetization direction from the surface normal, $K < 0$), where the z component of the total angular momentum (J) is denoted by J_z. These descriptions are linked by the correspondence principle $\cos \theta = J_z/J$. At spin-flip events, the magnetization direction of the object can be changed through the exchange of spin angular momentum with the tunneling electrons. The relationship between the MAE and the spin-flip excitation can be accurately described with a recently proposed relativistic model.[8] In the relativistic model, the spin-flip of tunneling electrons excites the ground state of magnetic clusters with $J_z = \pm J$ to the state with $J_z = \pm (J - 1)$. The inelastic spin-flip excitation energy E_{sf} corresponds to the energy difference between these two states. Hence, one can estimate the classical MAE K as $E_{sf} \times J^2/(2J - 1)$ with known J. Since the inelastic spin-flip excitation feature, appearing as a kink in the tunneling current I as a function of the bias voltage V in the low bias regime, is usually too weak to be identified,[9] the second derivative of the tunneling current (d^2I/dV^2), showing a peak is presented here. This excitation occurs for both tunneling directions, resulting in a positive (negative) peak structure at a positive (negative) bias.[10]

Before describing the experimental results, we investigated the electronic and magnetic properties of Gd atoms on Pt(111) and Cu(111) using our *ab initio* fully relativistic Green function method designed for clusters in real-space embedded in semi-infinite layered systems.[11] The atomic positions of Gd and surrounded atoms of the substrates were determined by means of the VASP code, well-known for providing precise total energies and forces.[12,13] The calculations show that Gd atoms do not penetrate deep inside the surface and experience inward relaxations of 0.20 Å and 0.12 Å on Pt(111) and Cu(111) surfaces, respectively. To describe the localized 4*f* electrons of Gd correctly, we applied a self-interaction correction method implemented within the multiple-scattering theory.[14,15] Contrary to the conventional local density approximation of the density functional theory (DFT), this first-principles approach is specially designed to describe localized electrons within the standard DFT removing a spurious self-interaction of an electron with itself. In particular, the self-interaction correction method reproduces correctly structural, electronic, and magnetic properties of lanthanide series.[16]

Interestingly, the calculations show little perturbation of the substrate electronic density, indicating a weaker hybridization with the host materials than in the case of 3*d* adatoms on Pt(111).[2] The calculated magnetic moments of Gd on hcp and fcc absorption sites with surrounding Pt and Cu atoms are shown in Figure 2. The magnetic moment of Gd is about 7 μ_B

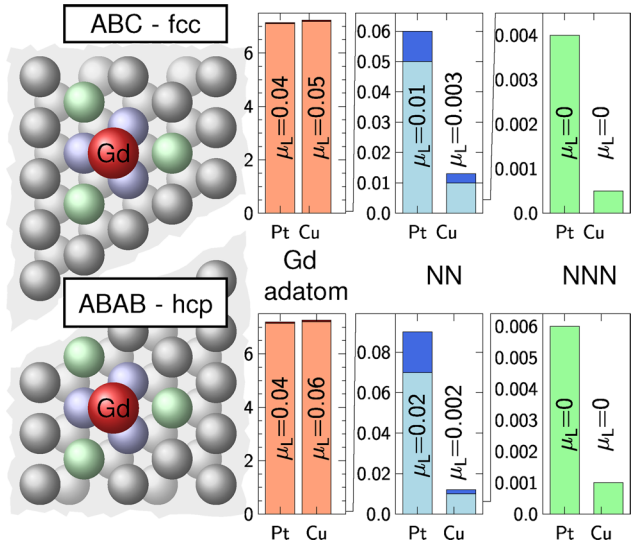

Figure 2. Magnetic spin and orbital moments of the Gd atoms (red spheres) and the surface atoms of the first (blue spheres) and second shell (green spheres) for the Pt(111) or Cu(111) surface: fcc stacking (upper panel) or hcp stacking (lower panel). The darker colors in the bar chart indicate the orbital moment μ_L.

on both substrates and for both adsorption sites and consists almost entirely of the spin moment of Gd corresponding to the well-known $S = 7/2$ state of Gd. The induced magnetic moments of surrounding Pt and Cu atoms are very small due to small overlap of the wave functions of the Gd atoms with the host. Thus, in the following experiments, we use the theoretical value of $J = 7/2$ for Gd atoms in good agreement with literature showing that, in a metallic environment, the Gd atom is present in an ionic Gd^{3+} state[17] with $J = 7/2$ obtained with Hund's rules ($S = 7/2$, $L = 0$).

The experimental d^2I/dV^2 spectra were recorded on Gd atoms and the bare Pt(111) surface in Figure 3a using a lock-in technique with 3 mV, 16.4 kHz modulated bias voltage. While the spectrum of the Gd atom clearly shows positive and negative peaks (Figure 3b), the Pt spectrum displays only a minute signal (Figure 3c). The genuine spectrum of the atom was obtained by subtracting the Pt background spectrum from the atom spectrum (Figure 3d). The spectrum is almost antisymmetric with a maximum and a minimum at the energies of ±5.2 meV. The same procedure gives the energies of ±4.5 meV for a Gd atom on Cu(111) as shown in Figure 3e. Owing

dx.doi.org/10.1021/nl302250n | *Nano Lett.* 2012, 12, 4805−4809

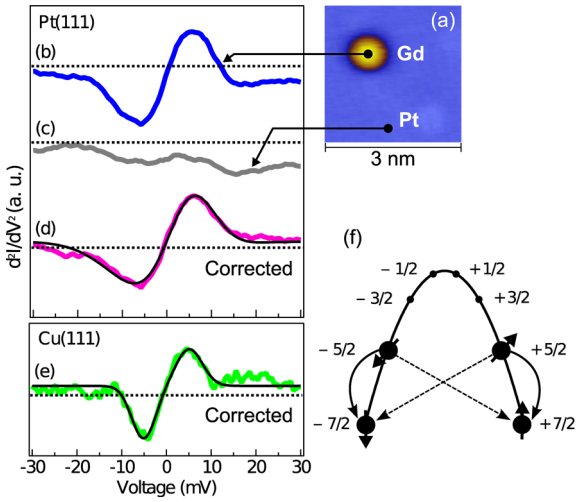

Figure 3. (a) Topography of a Gd atom on Pt(111). The d^2I/dV^2 spectra are recorded on (b) the Gd atom and (c) the bare Pt(111). Background-corrected d^2I/dV^2 spectra of the Gd atom on (d) Pt(111) and (e) Cu(111). The black solid lines give Gaussian fits. (f) Relaxation mechanism of a Gd atom on the surface with the 3-fold-rotational symmetry. Without in-plane anisotropy terms, relaxation channels shown by solid arrows are dominant. With in-plane anisotropy terms additional relaxation channels are shown by dotted arrows.

to the similar energies and excitation propabilities (8% and 5% on Pt and Cu, respectively), the same origin of the observed peaks and dips in the d^2I/dV^2 spectra is expected. Interestingly, the probability for spin excitations of Gd atoms is in the same range as the measured one on 3*d* elements.[2] This indicates that the coupling strength to the tunneling electrons is similar in both cases, that is, ITS can even detect spin excitations of strongly localized spins in the 4*f* orbitals. For Gd, there are two excitation processes possible: directly to the 4*f* orbitals or indirectly via the 5*d* orbital which is strongly coupled to the 4*f* orbitals by intraatomic exchange.[18]

Using a J of 7/2 and the measured E_{sf}, the MAEs of a Gd atom on Pt(111) and Cu(111) are estimated to be 10.6 and 9.2 meV/atom with the relativistic model, respectively. Note that the MAE cannot be attributed to the spin−orbit interaction of only the 4*f*-electrons, since their orbital moment is practically zero. The MAE originates from the interaction of the 4*f* electrons with a 5*d* electron of Gd, which is hybridized with the substrate.[19−21] Magnetism of 3*d* transition metal atoms strongly depends on the supporting surface. For example, while a Co atom shows a strong out-of-plane uniaxial anisotropy with a large MAE on Pt(111),[1,2] magnetic moments are quenched due to the Kondo screening on Cu(111).[22] This drastic change of magnetism is due to the strong hybridization of 3*d* states with the surfaces. In contrast to transition metal atoms, magnetism of rare earth atoms is robust against variations of the surfaces since the strongly localized 4*f* states hybridize less with surfaces. Hence, the similar MAEs of Gd atoms on Pt(111) and Cu(111) are reasonable and ensure again the spin-flip excitation as the origin of observed features in the d^2I/dV^2 spectra. On both used surfaces, two different adsorption sites are present. Thus, the Gd atom can sit either on a hcp or a fcc adsorption site. Experimentally, no significant difference in the MAE was observed within the variation of the MAE due to influences of the local density of states (LDOS) of the substrates.[2,23]

We also calculated the MAE from ab initio as function of the adsorption sites of the atom and the substrate. For Gd on Pt(111), 9.5 and 8.9 meV are determined for fcc and hcp sites, respectively, on Cu(111) 8.7 and 8.1 meV for fcc and hcp sites, respectively. These values agree very well with the experimental values, show the same trend of slightly lower MAEs for atoms on Cu(111), and only weakly depend on the absorption site. The latter confirms the absence of differences in the MAEs for hcp and fcc sites in the experiment. This is in contrast to the magnetic properties of 3*d* atoms on Pt(111), where the magnetic properties depend strongly on the adsorption site.[2,8] Thus, the magnetic properties of Gd on metallic surfaces are much more robust against the local environment and the electronic structure of the substrate.

The ITS spectra shown in Figure 3 reflect the spin excitations from ground states $|J = 7/2, J_z = \pm 7/2\rangle$ to the first excited states $|7/2, \pm 5/2\rangle$. Lifetimes of these excited states τ can be extracted from the widths of the peaks in the spectra. The relationship between this lifetime and the intrinsic width of the spectrum W_{in} is expressed by the uncertainty principle $\tau W_{in} \geq \hbar/2$. W_{in} is given by the subtraction of instrumental broadening effects of the temperature T and the modulation voltage V_{mod} from the measured width W ($W_{in} \sim [W^2 - (5.4kT)^2 - (1.7eV_{mod})^2]^{1/2}$).[9] After subtracting the instrumental broadening, the lifetimes of Gd atoms on Pt and Cu are found to be 100 and 160 fs, respectively. These determined values are significantly longer than the observed ones in 3*d* atoms on metallic substrates,[2,8] due to strongly localized 4*f* states. However, the strong exchange of the 4*f* states to the 5*d* states opens an efficient intra-atomic relaxation process.[18] Additionally, the 3-fold-rotational symmetry of Pt(111) and Cu(111) surfaces could result in in-plane MAE terms of third or sixth order ($J_+^6 + J_-^6$). With the sixth order in-plane anisotropy term, the first excited states $|7/2, \pm 5/2\rangle$ can couple to the other ground states $|7/2, \mp 7/2\rangle$. This coupling opens additional relaxation channels via magnetization tunneling as shown by dotted arrows in Figure 3f. This, in turn, would lead to a shortening of the lifetimes caused by increased relaxation probabilities.

The MAEs and lifetimes of Gd atoms on Pt(111) and Cu(111) surfaces are summarized in Table 1. Although the differences are small, one might notice the relationship between evaluated MAEs and lifetimes relative to the supported surface. The Gd atoms on the Pt(111) surface show slightly higher MAE but shorter lifetimes than on the Cu(111) surface. This tendency can be attributed to a higher LDOS at the Fermi energy of Pt(111),[24] which can hybridize with the 5*d* states. On the one hand, this increases the magnetic anisotropy which the 4*f* states experience. On the other hand the stronger hybridization reduces the lifetime of the excited states. Since the relaxation mechanism is driven by electron−electron scattering of the Gd electrons and the substrate electrons, the lifetime depends on the density of states of the substrate, and therfore a slightly shorter lifetime of the excited state of Gd on Pt(111) than on Cu(111) is expected. This is in agreement with ITS measurements of Fe atoms on Pt(111), which

Table 1. Obtained MAEs and Lifetimes of Gd Atoms

surface	E_{sf} (meV)	MAE (meV)	$\|D\|$ (meV)	τ (fs)
Cu(111)	4.5 ± 0.3	9.2 ± 0.4	0.75 ± 0.03	160 ± 80
Pt(111)	5.2 ± 0.3	10.6 ± 0.4	0.86 ± 0.03	100 ± 20

dx.doi.org/10.1021/nl302250n | *Nano Lett.* 2012, 12, 4805−4809

revealed a higher MAE but shorter lifetime than Fe atoms on Cu(111).[2,23]

Investigations of magnetic excitations of Gd were extended to clusters with the atomic manipulation capabilities of the STM, resulting in both Gd atoms on nearest neighbor position of the same stacking (fcc-fcc or hcp-hcp). We found that the strongly localized character of the 4*f* states persists in a Gd dimer. In addition to the MAE, ITS can probe the exchange interaction in the Gd dimer. The dimer has two excited states, that is, the collinear and noncollinear excited states.[2,3] Indeed, the d^2I/dV^2 spectra of Gd dimers on Pt(111) and Cu(111) show two inelastic excitations as revealed in Figure 4a.

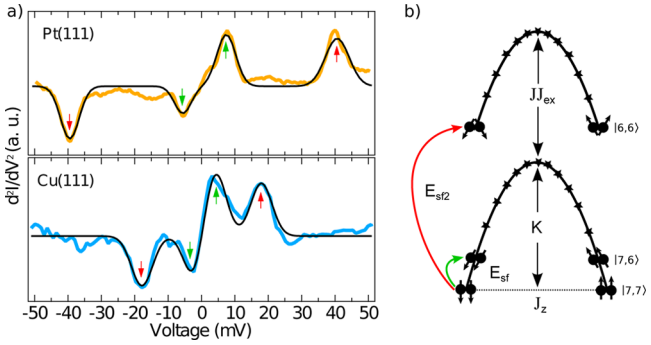

Figure 4. (a) Background-corrected d^2I/dV^2 spectra of Gd dimers on Pt(111) and Cu(111) showing two inelastic excitations indicated by arrows. The black solid line gives Gaussian fit. (b) The lowest two multiplets of a Gd dimer including the excitation passes to the collinear (green arrow) and noncollinear (red arrow) excitation.

Assuming a ferromagnetic coupling, the collinear excitation E_{sf} is within the largest multiplet ($J = 7$) and related to the MAE of the dimer. The noncollinear excitation E_{sf2} into a smaller multiplet ($J = 6$) is the sum of the MAE and the exchange energy J_{ex} (cf. Figure 4b). Besides the MAE ($|D|$) obtained from E_{sf}, J_{ex} can be calculated from $E_{sf2} = J_{ex} - 13D$.[3] The determined MAE and J_{ex} of the Gd dimers are shown in Table 2. While the MAE of Gd on Cu(111) decreases slightly with the cluster size, the MAE on Pt(111) increases. In contrast to a rapid drop of the MAE with the cluster size in 3*d* transition metals,[1,2] the MAE of the Gd dimer shows a similar value as the single Gd atom. This is in line with the above-discussed mechanism that the MAE is caused by an intra-atomic exchange between the 5*d* and 4*f* electrons of Gd. Thus, forming a dimer affects the MAE per atom only minutely. This robustness of the MAE per atom is a very significant advantage of rare earth clusters, as it would allow to form larger clusters without loss of MAE. Thus, by increasing the cluster size, the magnetic stability of the cluster caused by the MAE should rise linearly in contrast to that of 3*d* metal clusters.

The exchange constants for the Gd dimer on Pt and Cu are determined to be 4.8 and 1.96 meV/$\hbar^2$, respectively. The values strongly depend on the substrates in contrast to the MAEs. Since the two localized 4*f* orbitals of the dimers do not hybridize directly, exchange is only mediated by the indirect Ruderman–Kittel–Kasuya–Yosida coupling via the substrate electrons.[25−28] Thus, the LDOS at the Fermi level of the substrates largely determines the exchange constant, revealing a much larger value for a Gd dimer on Pt(111) than on Cu(111). The J_{ex} of the Gd dimers shows much smaller values compared to that of 3*d* transition metal dimers[2,3,29] (e.g., Fe dimer: 12 meV/$\hbar^2$, Co dimer: 14 meV/$\hbar^2$) as expected from the indirect coupling of the 4*f* states. The values for J_{ex} of the Gd dimer are in reasonable agreement with the exchange of J_{ex} of ∼1.3 meV/$\hbar^2$ deduced from Curie temperature of bulk Gd (292 K). The excitation probabilities into the collinear and the noncollinear states give similar values for each substrate, which can be fully explained with the spin-flip excitations described by the relativistic model.[8] Ab initio calculations were performed to investigate the dimers. The most stable configuration of the dimer is the state with both atoms adsorbed on neighboring hcp sites, in agreement with the experimental results. In this configuration, the two atoms couple ferromagnetically with J_{ex} = 1.4 meV/$\hbar^2$ and 0.98 meV/$\hbar^2$ for Pt(111) and Cu(111), respectively. Thus the calculations show the same trend as the experiment with respect to the variation of the substrate. Lifetimes of the collinear (noncollinear) states of the dimer are evaluated to be 90 ± 10 fs (71 ± 4 fs) and 122 ± 33 fs (106 ± 9 fs) for Pt(111) and Cu(111), respectively. Interestingly, these lifetimes are similar to the lifetime of single Gd atoms, which is not the case for the 3*d* transition metal dimers. Especially for the noncollinear state, the lifetimes of the 3*d* elements were extremely short due to the strong exchange interaction.[2,3,29] The observed tendency of longer lifetimes of the Gd dimer can be directly related to the smaller J_{ex}; that is, the dimer almost behaves as two isolated atoms.

In conclusion, we investigate the magnetic anisotropy and the magnetization dynamics of rare earth atoms and dimers as well as the exchange of the dimer. ITS measurements have revealed that spin excitations of 4*f* electrons are feasible and the anisotropy and the lifetime of Gd are robust with respect to the changes of the supporting surface or size of the cluster. Additionally, a strong dependence of J_{ex} due to the indirect interaction between the 4*f* shells is observed. The anisotropy per 4*f* atom does not drop significantly with cluster size potentially leading to stable spin clusters at cryogenic temperatures. The quantum nature of the spins in the localized 4*f* states will open up new possibilities to realize atomically small magnetic bits possibly as building blocks for quantum bits easily accessible by STM.

AUTHOR INFORMATION

Corresponding Author

*E-mail: wulf.wulfhekel@kit.edu.

Notes

The authors declare no competing financial interest.

ACKNOWLEDGMENTS

We thank J. Henk and H. Mirhosseini for insightful discussions. Funding from the Deutsche Forschungsgemeinschaft is

Table 2. Obtained MAEs and Exchange Constants of Gd Dimers

substrate	E_{sf} (meV)	MAE (meV/atom)	$\|D\|$ (meV)	E_{sf2} (meV)	J_{ex} (meV/$\hbar^2$)
Pt(111)	6.5 ± 0.2	12.3 ± 0.4	0.50 ± 0.02	40.0 ± 0.2	4.79 ± 0.02
Cu(111)	4.2 ± 0.2	7.9 ± 0.4	0.32 ± 0.02	17.9 ± 0.1	1.96 ± 0.02

acknowledged by W.W (DFG grant WU 349/4-2) and A. E (DFG grant 340/4-1).

REFERENCES

(1) Gambardella, P.; Rusponi, S.; Veronese, M.; Dhesi, S. S.; Grazioli, C.; Dallmeyer, A.; Cabria, I.; Zeller, R.; Dederichs, P. H.; Kern, K.; Carbone, C.; Brune, H. *Science* **2003**, *300*, 1130−1133.
(2) Balashov, T.; Schuh, T.; Takács, A. F.; Ernst, A.; Ostanin, S.; Henk, J.; Mertig, I.; Bruno, P.; Miyamachi, T.; Suga, S.; Wulfhekel, W. *Phys. Rev. Lett.* **2009**, *102*, 257203.
(3) Schuh, T.; Balashov, T.; Miyamachi, T.; Takács, A. F.; Suga, S.; Wulfhekel, W. *J. Appl. Phys.* **2010**, *107*, 09E156.
(4) Heinrich, A. J.; Gupta, J. A.; Lutz, C. P.; Eigler, D. M. *Science* **2004**, *306*, 466−469.
(5) Hirjibehedin, C. F.; Lin, C.-Y.; Otte, A. F.; Ternes, M.; Lutz, C. P.; Jones, B. A.; Heinrich, A. J. *Science* **2007**, *317*, 1199−1203.
(6) Loth, S; Etzkorn, M; Lutz, C. P.; Eigler, D. M.; Heinrich, A. J. *Science* **2010**, *329*, 1628−1630.
(7) Eigler, D. M.; Schweizer, E. K. *Nature* **1990**, *344*, 524−526.
(8) Schuh, T.; Balashov, T.; Miyamachi, T.; Wu, S.; Kuo, C.; Ernst, A.; Henk, J.; Wulfhekel, W. *Phys. Rev. B* **2011**, *84*, 104401.
(9) Stipe, B. C.; Razaei, M. A.; Ho, W. *Science* **1998**, *280*, 1732−1735.
(10) Wolf, E. *Principles of Electron Tunneling Spectroscopy*; Oxford University Press: New York, 1989; p 592.
(11) Lüders, M.; Ernst, A.; Temmerman, W. M.; Szotek, Z.; Durham, P. J. *J. Phys.: Condens. Matter* **2001**, *13*, 8587−8606.
(12) Kresse, G.; Hafner, J. *Phys. Rev. B* **1994**, *49*, 14251−14269.
(13) Kresse, G.; Furthmüller, J. *Phys. Rev. B* **1996**, *54*, 11169−11186.
(14) Perdew, J. P.; Zunger, A. *Phys. Rev. B* **1981**, *23*, 5048.
(15) Lüders, M.; Ernst, A.; Däne, M.; Szotek, Z.; Svane, A.; Ködderitzsch, D.; Hergert, W.; Györffy, B. L.; Temmerman, W. M. *Phys. Rev. B* **2005**, *71*, 205109.
(16) Hughes, I. D.; Däne, M.; Ernst, A.; Hergert, W.; Lüders, M.; Poulter, J.; Staunton, J. B.; Svane, A.; Temmerman, W. M. *Nature* **2007**, *446*, 650.
(17) Hardiman, M.; Pellisson, J.; Barnes, S.; Bisson, P.; Peter, M. *Phys. Rev. B* **1980**, *22*, 2175−2194.
(18) Wietstruk, M.; Melnikov, A.; Stamm, C.; Kachel, T.; Pontius, N.; Sultan, M.; Gahl, C.; Weinelt, M.; Dürr, H.; Bovensiepen, U. *Phys. Rev. Lett.* **2011**, *106*, 127401.
(19) Franse, J.; Gersdorf, R. *Phys. Rev. Lett.* **1980**, *45*, 50−53.
(20) Colarieti-Tosti, M.; Simak, S.; Ahuja, R.; Nordström, L.; Eriksson, O.; Åberg, D.; Edvardsson, S.; Brooks, M. *Phys. Rev. Lett.* **1980**, *45*, 50−53.
(21) Abdelouahed, S.; Alouani, M. *Phys. Rev. B* **2009**, *79*, 054406.
(22) Knorr, N.; Schneider, M. A.; Diekhner, L.; Wahl, P.; Kern, K. *Phys. Rev. Lett.* **2002**, *88*, 96804.
(23) Khajetoorians, A.; Lounis, S.; Chilian, B.; Costa, A.; Zhou, L.; Mills, D.; Wiebe, J.; Wiesendanger, R. *Phys. Rev. Lett.* **2011**, *106*, 037205.
(24) Sigalas, M.; Papaconstantopoulos, D. A.; Bacalis, N. C. *Phys. Rev. B* **1992**, *45*, 5777−5783.
(25) Ruderman, M. A.; Kittel, C. *Phys. Rev.* **1954**, *96*, 99−102.
(26) Kasuya, T. *Prog. Theor. Phys.* **1956**, *106*, 893−898.
(27) Yosida, K. *Phys. Rev.* **1957**, *106*, 893−898.
(28) Zhou, L.; Wiebe, J.; Lounis, S.; Vedmedenko, E.; Meier, F.; Blügel, S.; Dederichs, P. H.; Wiesendanger, R. *Nat. Phys.* **2010**, *6*, 187−191.
(29) Miyamachi, T.; Schuh, T.; Balashov, T.; Suga, S.; Wulfhekel, W. *e-J. Surf. Sci. Nanotechnol.* **2011**, *9*, 237−240.